Rice Morphology Determinant-Mediated Actin Filament Organization Contributes to Pollen Tube Growth[1][OPEN]

Gang Li,[a,2] Xiujuan Yang,[a,2] Xiaoqing Zhang,[b] Yu Song,[b] Wanqi Liang,[b] and Dabing Zhang[a,b,3]

[a]University of Adelaide-Shanghai Jiao Tong University Joint Laboratory for Plant Science and Breeding, School of Agriculture, Food, and Wine, University of Adelaide, Waite Campus, Urrbrae, South Australia 5064, Australia

[b]Joint International Research Laboratory of Metabolic and Developmental Sciences, Shanghai Jiao Tong University-University of Adelaide Joint Centre for Agriculture and Health, School of Life Sciences and Biotechnology, Shanghai Jiao Tong University, Shanghai 200240, China

ORCID IDs: 0000-0002-1744-5220 (G.L.); 0000-0001-9340-3551 (X.Y.); 0000-0001-6988-034X (Y.S.); 0000-0002-9938-5793 (W.L.); 0000-0003-3181-9812 (D.Z.).

For successful fertilization in angiosperms, rapid tip growth in pollen tubes delivers the male gamete into the ovules. The actin-binding protein-mediated organization of the actin cytoskeleton within the pollen tube plays a crucial role in this polarized process. However, the mechanism underlying the polarity of the actin filament (F-actin) array and behaviors in pollen tube growth remain largely unknown. Here, we demonstrate that an actin-organizing protein, Rice Morphology Determinant (RMD), a type II formin from rice (*Oryza sativa*), controls pollen tube growth by modulating the polarity and distribution of the F-actin array. The rice *rmd* mutant exhibits abnormal pollen tube growth and a decreased germination rate of the pollen grain in vitro and in vivo. The *rmd* pollen tubes display a disorganized F-actin pattern with disrupted apical actin density and shank longitudinal cable direction/arrangement, indicating the novel role of RMD in F-actin polarity during tip growth. Consistent with this role, RMD localizes at the tip of the rice pollen tube, which is essential for pollen tube growth and polarity as well as F-actin organization. Furthermore, the direction and characteristics of the RMD-guided F-actin array positively regulate the deposition of cell wall components and the pattern and velocity of cytoplasmic streaming during rice pollen tube growth. Collectively, our results suggest that RMD is essential for the spatial regulation of pollen tube growth via modulating F-actin organization and array orientation in rice. This work provides insights into tip-focused cell growth and polarity.

Tip growth, an extreme form of polarized growth, is crucial for the development and morphogenesis of eukaryotic organisms. Extension of the cell wall occurring at a single site on the cell surface produces a cylinder-shaped cell. Rapid tip growth is associated with responses to external and intracellular signals that guide the direction of growth toward a specific goal (Lowery and Van Vactor, 2009; Berepiki et al., 2011; Rounds and Bezanilla, 2013). The pollen tube acts as a conduit connecting the pollen grain and ovule to enable double fertilization in higher plants and has been regarded as an ideal system for investigating the molecular mechanisms underlying polarized cell growth.

Pollen tubes are divided into three regions: the apex or apical dome, which is a growth region denoting the hemisphere-shaped tip of the cell; the subapex, which is a transition region; and the shank, mimicking that of ordinary plant cells containing the typical repertoire of organelles (Geitmann and Emons, 2000; Cai and Cresti, 2009). Generally, the rapid growth of a single pollen tube cell without cell division occurs exclusively at the tip and is associated with well-organized cytoplasmic streaming and the movement of organelles in the shank region. During pollen tube extension, the growth direction is reoriented continuously by internal signals and cell wall composition. At the apical region, the tip growth of pollen tubes requires the fusion of secretory vesicles consisting of Golgi-derived cell wall components with the plasma membrane (PM), and this process is balanced by the endocytic recycling of membrane materials (Hepler and Winship, 2015;

[1] This work was supported by National Key Technologies Research and Development Program of China, Ministry of Science and Technology (grant nos. 2016YFD 0100804 and 2016YFE0101000), National Natural Science Foundation of China (grant nos. 31430009, 31230051, 31322040, and 31271698), an Australia-China Science and Research Fund Joint Research Centre grant ACSRF48187, the start-up funding (13114779 and 62117250) for D.Z. from the School of Agriculture, Food, and Wine, University of Adelaide, and the Innovative Research Team, Ministry of Education, the 111 Project (grant no. B14016).

[2] These authors contributed equally to the article.

[3] Address correspondence to dabing.zhang@adelaide.edu.au.

The author responsible for distribution of materials integral to the findings presented in this article in accordance with the policy described in the Instructions for Authors (www.plantphysiol.org) is: Dabing Zhang (dabing.zhang@adelaide.edu.au).

G.L. and D.Z. designed the project; G.L. and X.Y. performed most of the experiments and analyzed the results; X.Z. and Y.S. performed plasmid construction and collected the materials; G.L., X.Y., W.L., and D.Z. wrote and revised the article.

[OPEN] Articles can be viewed without a subscription.

www.plantphysiol.org/cgi/doi/10.1104/pp.17.01759

Grebnev et al., 2017; Qu et al., 2017). The vesicles within pollen tubes contain mostly pectin, especially homogalacturonans, which are a major component of the cell wall at the pollen tube tip (Geitmann and Steer, 2006; Winship et al., 2010; Chebli et al., 2012). Highly methoxylated homogalacturonans are accumulated at the apical region through exocytosis to loosen the cell wall and form the thick, soft tip wall with a lower stress-yield point, allowing the pollen tube to deform more easily. Thus, as the cell wall thickens, the polar growth rate increases in the direction of the tip (McKenna et al., 2009; Zerzour et al., 2009; Rojas et al., 2011; Rounds and Bezanilla, 2013). In this process, the bidirectional reverse-fountain cytoplasmic streaming between the shank region and the subapex is presumably essential to ensure a sufficient supply of materials required for cell expansion (Cheung and Wu, 2008; Grebnev et al., 2017).

The actin cytoskeleton is a pivotal determinant during pollen tube growth, providing molecular tracks for intracellular trafficking events to organize the patterning of the cell wall (Cheung and Wu, 2008; Qu et al., 2015). Distinct organization patterns of the actin cytoskeleton are present in different regions of the pollen tube to maintain the polarized growth of cells. In the shank region, longitudinal actin cables exist throughout the cytoplasm, facilitating the transport of organelles and vesicles between the shank region and the subapex to support the reverse-fountain cytoplasmic streaming pattern (Ye et al., 2009; Cheung et al., 2010; Zheng et al., 2013; Duckney et al., 2017; Qu et al., 2017). At the subapex, actin filaments form regular structures in different species, such as the collar, fringe, mesh, or funnel, and some observations indicated that subapical F-actin could regulate the accumulation of vesicles and the growth of the tip region (Gibbon et al., 1999; Fu et al., 2001; Vidali et al., 2001; Chen et al., 2002; Lovy-Wheeler et al., 2005; Qu et al., 2017). At the apex, actin filaments are generally less abundant but are highly dynamic with dense actin structures, which mediates the interaction between the apical/subapical PM and the cytoplasm during rapid tube elongation (Fu et al., 2001; Lee and Yang, 2008; Cai and Cresti, 2009; Cheung et al., 2010; Qu et al., 2013; Rounds et al., 2014; Zhou et al., 2015; Qu et al., 2017). Recently, Qu et al., (2017) demonstrated that F-actin originating from the apical membrane forms a specialized structure consisting of longitudinally aligned actin bundles at the cortex and inner cytoplasmic filaments with a distinct distribution, which plays a pivotal role in the regulation of the growth of the pollen tube tip in Arabidopsis (*Arabidopsis thaliana*).

Actin shapes and dynamics are modulated directly by several types of actin-binding proteins during pollen tube growth (Ren and Xiang, 2007; Staiger et al., 2010; Fu, 2015). In Arabidopsis and lily (*Lilium longiflorum*), fimbrins (FIM), domain of Lin11, Isl-1, and Mec-3 proteins, actin-depolymerizing factors, several formins, and villins (VLN) have been shown to be involved in the formation and maintenance of longitudinal actin cables in the shank region of pollen tubes (Wu et al., 2010; Zheng et al., 2013; Fu, 2015). VLN2, VLN5, AtFIM5, and LlFIM1 bundle apical PM-anchored F-actin and contribute to the formation of actin fringe or collar structures in the subapical region (Su et al., 2012; Qu et al., 2013; Zhang et al., 2016a). In the apex, several actin-binding proteins, including VLN and Rop-interactive CRIB Motif-containing Protein1, are implicated in the patterning of apical F-actin dynamics (Qu et al., 2013; Zhou et al., 2015). However, the mechanisms that maintain the dynamic polarity of longitudinal actin cables and facilitate the polarized recycling of shank-apex actin still remain elusive.

In flowering plants, formins are grouped into two subclasses, type I and type II, which are conserved in seed-producing plants and are expressed in tip-growing cells (Vidali et al., 2009; van Gisbergen and Bezanilla, 2013). Overexpression studies have suggested the roles of formins in actin cable formation and pollen tube growth in Arabidopsis (Cheung and Wu, 2004). RNA interference (RNAi) of two type I formins in Arabidopsis and tobacco (*Nicotiana tabacum*) indicated their involvement in pollen tube growth. The reduction of *Formin Homology3* (*AtFH3*) accumulation causes abolished actin cable formation in the shank region and altered cytoplasmic streaming, leading to shorter and wider cells (Ye et al., 2009). Decreased expression of *NtFH5* disrupts actin organization near the apex regions and results in the wavy growth of tobacco pollen tubes (Cheung et al., 2010). Overexpression of a lily pollen-specific type I formin, *LlFH1*, causes excessive actin cables in the pollen tube tip, and knockdown of *LlFH1* specifically decreases F-actin in the tube apex and actin fringe formation and results in reduced germination rate of pollen and average length of pollen tubes (Li et al., 2017). Further investigations showed that formins function as nucleation factors to stimulate actin assembly and actin cables in pollen tubes (Ye et al., 2009; Cheung et al., 2010; van Gisbergen and Bezanilla, 2013; Li et al., 2017). These studies indicate that type I formins participate in generating actin structures that facilitate and maintain the tip growth of the pollen tube. However, a loss-of-function study in the moss *Physcomitrella patens* demonstrated that type I formins, rather than contributing to polarized growth, are needed for efficient cytokinesis and that type II formins are essential for tip growth, although its underlying mechanism is not clear (Vidali et al., 2009; van Gisbergen et al., 2012).

Our previous work demonstrated that a type II formin protein, RICE MORPHOLOGY DETERMINANT (RMD; also called BENT UPPERMOST INTERNODE1) from rice (*Oryza sativa*), functionally regulates cytoskeleton organization by nucleating, capping, and bundling actin in vitro and also plays a crucial role in regulating F-actin dynamics and arrays in rice cells (Yang et al., 2011; Zhang et al., 2011; Li et al., 2014). *rmd* mutants exhibit altered microfilament and microtubule arrays, causing defective plant morphology (Zhang et al., 2011). In addition, RMD is a key regulator of the

auxin-actin self-organizing regulatory loop that controls the diffuse cell growth of rice roots (Li et al., 2014). However, the role of RMD-mediated F-actin organization in polarized cell growth is poorly understood. In this study, we demonstrated that RMD controls rice pollen tube growth by modulating the array orientation and distribution of F-actin. Furthermore, we showed that tip-localized RMD determines the deposition of pectin at the tube wall and the efficiency of cytoplasmic streaming in the shank of tubes. We conclude that RMD is a key player in controlling rice pollen tube growth through maintaining F-actin organization and array polarity.

RESULTS

RMD Promotes Pollen Tube Growth in Rice

Previously, we showed that RMD determines rice morphogenesis, including plant architecture and various organs (Zhang et al., 2011). Notably, *rmd* mutants displayed smaller pollen grains with reduced F-actin and aborted microtubule arrays compared with those of the wild type (Zhang et al., 2011), suggesting the possible role of RMD in pollen development. To test this hypothesis, we investigated the phenotypic features of the reproductive organs in the *rmd-1* mutant, which contains a null mutation of *RMD*. The *rmd-1* anther and pistil were shorter, approximately 76% of the size of the wild-type organs (Supplemental Fig. S1, A–D). Despite the defective development of the *rmd-1* anther, the *rmd-1* mutant was able to produce mature pollen grains. However, iodine-potassium iodide staining showed that the *rmd-1* mutant had a reduced proportion of mature pollen grains (~73.5%) compared with 94.2% in the wild type, suggesting the role of RMD in normal pollen development (Supplemental Fig. S1, E–G). Despite the change in panicle architecture, *rmd-1* and *rmd-2* (another mutant allele of *RMD*; Zhang et al., 2011) plants could generate seeds with a similar seed-setting rate to that of the wild type after fertilization (Supplemental Fig. S1, H–I), although the seed shape was altered in the mutants (Supplemental Fig. S1J). These observations indicate that RMD has a critical role in pollen development.

Although the loss of function of *RMD* did not cause obvious impaired fertilization, we asked whether *RMD* has a role in pollen tube growth. To achieve this goal, pollen grains from wild-type and *rmd-1* plants were germinated in liquid germination medium in vitro (Fig. 1, A and B). At 10 min after germination, the average pollen germination frequency of wild-type plants was about 80.6%, while that of the *rmd-1* mutant was about 65.4% ($P < 0.01$, Student's t test; Fig. 1C). We also compared the dimensions and growth rates of wild-type and *rmd-1* pollen tubes after germination in vitro. The average length of *rmd-1* pollen tubes was significantly lower than that of wild-type plants, while the average width of *rmd-1* pollen tubes was remarkably higher than that of wild-type plants (Fig. 1, D–G; $n > 150$ tubes of each), indicating a negative impact on pollen tube growth polarity in the *rmd-1* mutant. To reveal whether the shorter pollen tubes in the *rmd-1* mutant are caused by the delayed germination or growth, individual pollen grains growing on the germination medium were monitored using a light microscope (Supplemental Fig. S2). The average growth rate ($\pm$SD) of *rmd-1* pollen tubes was 3.87 ± 0.77 ($n = 36$) μm min^{-1} compared with 5.66 ± 1.09 ($n = 39$) μm min^{-1} for wild-type pollen tubes (Fig. 1H). These results demonstrate that the loss of function of *RMD* leads to inhibited pollen germination and pollen tube elongation in vitro.

To directly observe the behavior of pollen tube growth in vivo, pollen grains collected from wild-type and *rmd-1* plants were pollinated to wild-type pistils. As shown in Figure 2, *rmd-1* pollen tubes exhibited less activity compared with wild-type pollen tubes after attachment onto the pistil stigma (Fig. 2, A–D). Wild-type pollens could form fine pollen tubes 10 or 20 min after pollination (Fig. 2, A and B). By contrast, *rmd-1* pollen tubes seemed relatively slower in their growth rate and were twisted (Fig. 2, C and D). Unlike the wild-type pollen tubes, which penetrated through the style and reached the bottom of the pistils after 30 min of pollination (Fig. 2E), *rmd-1* pollen tubes merely penetrated into the style and reached halfway down the pistils (Fig. 2F), suggesting the delayed growth of *rmd-1* pollen tubes. Furthermore, consistent with the in vitro data, the relative pollen germination frequency of *rmd-1* pollen was 55.8%, which was remarkably lower than that of the wild type (91.5%) in vivo (Fig. 2G). Statistical analysis showed that the wild-type pollen tube growth rate reached 11.95 ± 2.61 μm min^{-1} ($n = 92$), while the rate of the *rmd-1* pollen tube was 6.87 ± 2.18 μm min^{-1} ($n = 95$; Fig. 2H). In addition, in vitro and in vivo arrays also showed that the *rmd-2* mutation caused inhibited pollen tube growth/elongation (Supplemental Figs. S2 and S3). Therefore, these observations demonstrate that RMD positively regulates pollen germination and pollen tube growth in rice. Even though loss of function of *RMD* caused abnormal pollen tube growth, the seed setting of the mutant seems normal, possibly due to the excessive number of pollen grains during fertilization (Supplemental Fig. S1I; Zhang et al., 2011). This observation also suggests the major role of RMD in rapid tip growth instead of fertilization.

Expression of *RMD* in the Pollen Tube

To further evaluate the function of *RMD* in pollen tube growth, we extracted total RNAs from the whole flower, lemma, palea, lodicule, pistil, anther, and mature pollen grains of wild-type plants. Using reverse transcription quantitative PCR (RT-qPCR) and semiquantitative RT-PCR with *UBIQUITIN* as an internal control (Fig. 3A), we observed that *RMD* transcripts were accumulated abundantly in the lemma, pistil, anther, and

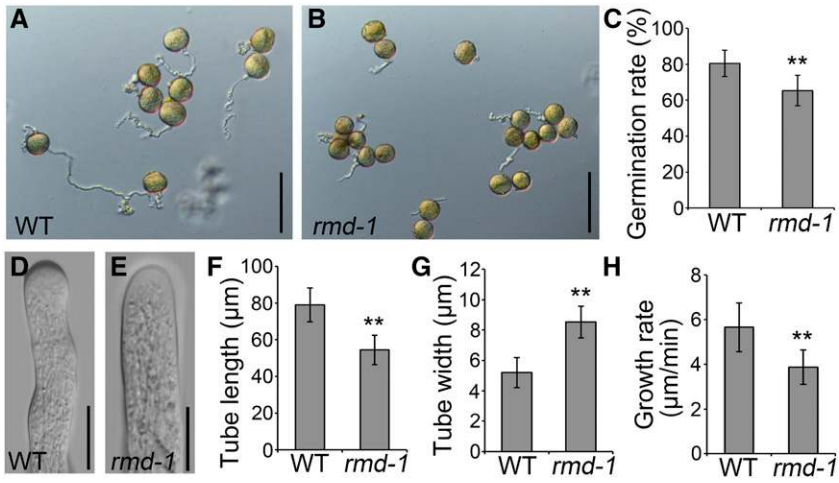

Figure 1. The *rmd-1* mutant has abnormal pollen germination and pollen tube growth in vitro. A and B, Micrographs of pollen tubes were taken 10 min after germination in vitro. Pollen grains derived from wild-type (WT; A) and *rmd-1* (B) plants were germinated in the standard liquid germination medium. Bars = 100 μm. C, In vitro germination percentages of wild-type and *rmd-1* pollen grains ($n > 200$ pollen grains for each genotype). D and E, Wild-type (D) and *rmd-1* (E) pollen tubes were visualized by a microscope 10 min after germination in vitro. Bars = 10 μm. F and G, The average pollen tube length (F) and width (G) of wild-type and *rmd-1* plants (only germinated pollen grains were taken into account) were analyzed 10 min after germination ($n >$ 150 for each genotype). H, Graph of pollen tube growth rates of the wild type and the *rmd-1* mutant between 3 and 10 min after germination in vitro (each genotype, $n > 35$). For C and F to H, error bars represent SD of at least three independent experiments. Student's *t* test: **, $P < 0.01$.

mature pollen (Fig. 3A). To confirm the expression pattern, we used previously obtained transgenic lines harboring the *RMD* promoter region fused with a reporter gene encoding GUS (Zhang et al., 2011). Histochemical staining of flower tissues from transgenic plants demonstrated high GUS activity in the pistil, anther wall, and pollen grains (Fig. 3, B and C).

To examine *RMD* expression in pollen and pollen tubes, we collected pollen grains from *proRMD*::*GUS* transgenic lines and observed a strong GUS signal in mature pollen grains (Fig. 3D). Next, we germinated *proRMD*::*GUS* pollen grains in vitro and clearly observed GUS signals in growing pollen tubes (Fig. 3, E–G). During the early stage of pollen germination, GUS signals were weak at the tip of *proRMD*::*GUS* pollen tubes (Fig. 3E, red arrow), but they were strong at the later stages, particularly at the pollen tube tip (Fig. 3, F and G, red arrows). This result supports that *RMD* has a function in pollen germination and pollen tube growth.

Localization of RMD in the Pollen Tube

In flowering plants, type II formins possess an N-terminal phosphatase and tensin-related (PTEN)-like domain, which is predicted to be associated with protein localization (Wang et al., 2012; van Gisbergen and Bezanilla, 2013). As a member of the type II formins, RMD contains the conserved PTEN-like domain followed by the formin homology1 (FH1) and FH2 domains (Fig. 4A) known to promote actin polymerization (Zhang et al., 2011). To investigate the function of RMD in pollen tube growth, we first analyzed its localization in growing pollen tubes of tobacco using transient expression. Assays of elongating tobacco pollen tubes expressing comparable levels of enhanced GFP (eGFP; control) driven by a pollen-specific *Lat52* promoter (*pLat52*; Twell et al., 1989) or RMD-eGFP driven by *pLat52* showed that RMD-eGFP accumulated predominantly at the tip region while the fluorescence of single GFP was distributed ubiquitously throughout the entire tube (Fig. 4B). To probe the role of the PTEN-like domain in the polarized localization of RMD, we investigated the eGFP signal fused with the PTEN-like domain and truncated RMD without the PTEN domain (FH1FH2-eGFP) in growing tobacco pollen tubes (Fig. 4B). Our result showed that PTEN-eGFP signals were localized at the tip of pollen tubes, mimicking RMD-eGFP, but the localization of FH1FH2-eGFP was in a nonpolar manner (Fig. 4B), indicating that the PTEN-like domain determines the tip localization of RMD in pollen tubes.

Subsequently, we observed the RMD localization in rice pollen grains and pollen tubes using transgenic lines of *RMD-eGFP* driven by the *RMD* native promoter in the *rmd-1* background (*proRMD*::*RMD-eGFP/rmd-1*). In the mature pollen grain, the presence of eGFP signals was polarized around the aperture of the pollen grain (Fig. 4C). In elongating pollen tubes in vitro, RMD showed the same apical localization as the transient assays in tobacco tubes (Fig. 4, B and C). In vivo pollinating assays of pollen grains on pistils also showed that RMD-eGFP signals existed at the tip zone of the tube (Fig. 4D). Together, RMD appears to be localized at the tip of pollen tubes, suggesting a role of RMD in organizing rice tip growth.

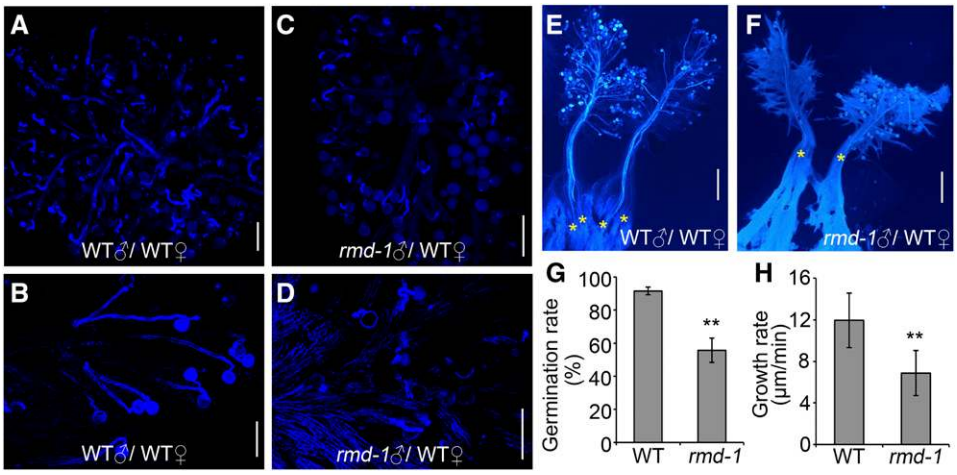

Figure 2. The *rmd-1* mutant has decreased pollen germination and inhibited pollen tube elongation in vivo. A to D, Wild-type (WT) pistils were hand pollinated with wild-type (A and B) and *rmd-1* (C and D) pollen grains, dissected after 10 min (A and C) and 20 min (B and D), and stained with Aniline Blue to visualize pollen tubes. Bars = 100 μm. E and F, Pollen grains from wild-type (E) and *rmd-1* (F) plants were used to pollinate wild-type pistils. Pollen tubes were visualized by Aniline Blue staining 30 min after pollination. Yellow asterisks represent pollen tubes that invaded the pistil. Bars = 500 μm. G, Germination percentages of wild-type and *rmd-1* pollen grains were measured 20 min after pollinating wild-type pistils. Over 300 pollen grains from at least 20 pistils were observed for each experiment. H, In vivo relative pollen tube growth rates were calculated 10 to 20 min after pollination as mentioned in E and F. At least 90 tubes of 15 pistils were observed for each genotype. For G and H, error bars represent SD of at least three experiments. Student's *t* test: **, $P < 0.01$.

RMD Controls F-Actin Distribution and Polarity in the Pollen Tube

Our previous studies demonstrated that RMD is an actin-binding protein that regulates actin polymerization, nucleating, capping, and bundling in vitro. In addition, RMD determines the F-actin organization and network in rice root cells (Zhang et al., 2011; Li et al., 2014). To determine the role of RMD in regulating F-actin organization and distribution in pollen tubes, we first observed F-actin arrays in wild-type and *rmd-1* mature pollen grains using staining with Alexa Fluor 488-phalloidin (Supplemental Fig. S4A). Actin filaments were seen throughout wild-type pollen grains, and strongly bundled actin filaments were observed around the apertures of grains. By contrast, random and weak signals of actin filaments were detected in *rmd-1* pollen grains, and there was no obvious accumulation of F-actin around the apertures (Supplemental Fig. S4A). The abnormal F-actin distribution in *rmd-1* pollen grains implies that RMD has a role in regulating pollen germination.

Furthermore, the *rmd-1*, *rmd-2*, and *proRMD*::*RMD-eGFP/rmd-1* (complementary) lines were used for the observation of F-actin organization and polarity in growing rice pollen tubes. In wild-type pollen tubes, F-actin was observed in diverse structures, depending on the locations within tubes. Specifically, F-actin was present at the tip region with a high density, while it formed a polarized longitudinal actin cable extending throughout the shank region (Fig. 5A; Supplemental Fig. S4B). By contrast, the distribution of F-actin in *rmd-1* and *rmd-2* pollen tubes appeared more spiral, predominantly as a transverse F-actin cable in the shank region (Fig. 5A; Supplemental Fig. S4B). In particular, the direction of actin cables in the shank of *rmd-1* pollen tubes showed an approximately vertical rotation compared with that of the wild type, and the initiation of the actin cable was depolarized at the apical zone of the tubes rather than in a longitudinal direction (Fig. 5A; Supplemental Fig. S4B). In addition, the expression of *RMD* driven by its own promoter (in the complementary lines) could rescue the F-actin phenotype of *rmd-1* pollen tubes (Supplemental Fig. S4B). These observations suggest that RMD determines the behavior and direction of F-actin in rice pollen tubes.

To quantify the extent of actin filament density in pollen tubes, fluorescence intensity and skewness were measured as described previously by Li et al. (2014). A statistical analysis of fluorescence intensity showed a higher density of F-actin in the shank region of *rmd-1* (n = 36) and *rmd-2* (n = 31) pollen tubes, while a lower density of F-actin was observed at the tip region of *rmd* pollen tubes compared with that of the wild type (n = 32; Fig. 5, B and C). Furthermore, more actin bundles existed in the subapical/tip domes of *rmd* pollen tubes, as indicated by the dramatic increase of mean skewness compared with that of the wild type, while the extent of actin filament bundling in the shank region of the *rmd-1* pollen tube was lower than that in wild-type tubes (Supplemental Fig. S4C), further demonstrating that the distribution pattern of F-actin in *rmd* pollen tubes is altered. To quantitatively evaluate the polarity of longitudinal actin cables, we determined the angles formed between actin cables and the elongation axis of

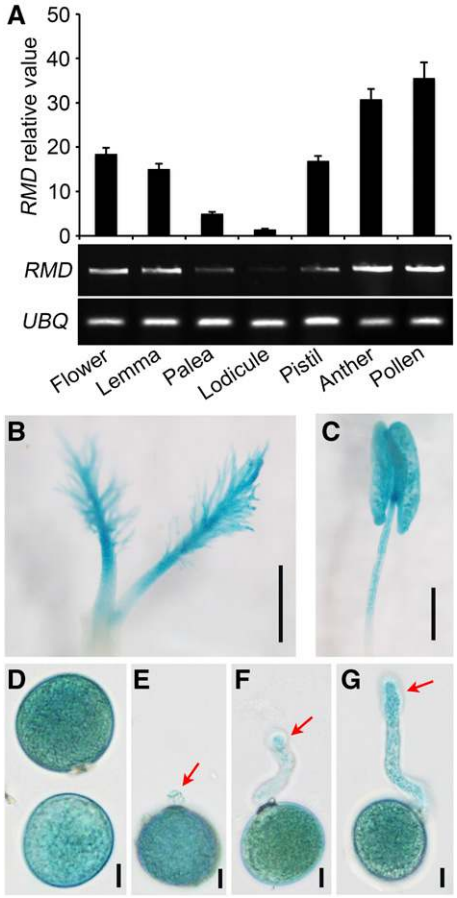

Figure 3. *RMD* is expressed in flower organs, pollen, and pollen tubes. A, Transcriptional analysis of *RMD* by RT-qPCR (top) and RT-PCR (bottom) in rice reproductive organs. *UBIQUITIN* (*UBQ*) served as a control. Error bars represent SD. Each reaction had three biological repeats. B and C, Promoter activities of *RMD* in the pistil (B) and anther (C) of the *proRMD*::*GUS* transgenic line. Bars = 500 μm (B) and 1 mm (C). D, Strong GUS signals were seen in pollen grains. Bar = 10 μm. E to G, GUS assay of *proRMD*::*GUS* pollen tubes. Pollen tubes were grown on liquid medium in vitro for 5 to 10 min. GUS signals were observed 24 h after staining. Red arrows indicate GUS signals in pollen tubes of different stages. Bars = 10 μm.

the pollen tube (Fig. 5B). These angles in the shank of wild-type pollen tubes were generally less than 20°, and only 5% of angles were determined to be larger than 60°. However, in *rmd* pollen tubes, the angles were increased dramatically, with over half of the actin cables forming greater than 60° angles with the elongation axis, some even larger than 70° ($n > 130$ actin cables of each; Fig. 5, B and D; Supplemental Fig. S4D). We also measured the maximum length of single cables of F-actin filaments elongated from the apical to the shank regions of the pollen tubes (n = ~100 actin filaments from 20 pollen tubes per line). These data showed that the maximum length of F-actin cables was shorter in *rmd-1* pollen tubes compared with those of the wild type (Fig. 5E). The F-actin density and cable direction in pollen tubes of the *proRMD*::*RMD-eGFP/rmd-1* complementary lines showed similar patterns and levels to those of wild-type tubes (Supplemental Fig. S4, B–D). Hence, these data suggest that RMD is required for the proper organization of actin cables in the shank and the normal F-actin density at the tip of pollen tubes.

Pollen Tube Growth and F-Actin Are Hypersensitive to Latrunculin B in the *rmd* Mutant

To assess the role of actin in RMD-dependent pollen germination and pollen tube growth, we next sought to test the effects of latrunculin B (LatB; an actin-polymerizing inhibitor) treatment in the *rmd* mutant. Pollen grains from wild-type plants and *rmd-1* mutants were germinated on a medium containing serial concentrations of LatB. The germination percentage of wild-type pollen grains was affected slightly by the concentration of LatB below 1 nM (Supplemental Fig. S5A). However, the pollen germination percentage of the *rmd-1* mutant decreased in a dose-dependent manner starting at 0.5 nM LatB (Supplemental Fig. S5A). Additionally, in vitro application of LatB showed that the growth rate of both wild-type and *rmd-1* pollen tubes was inhibited by treatment with LatB in a dose-dependent manner (Supplemental Fig. S5, B and C). Most wild-type pollen tube growth showed half-maximal inhibition at ~4 nM LatB. In contrast, the growth rate of *rmd-1* pollen tubes was affected severely at lower concentrations of LatB, and the half-maximal inhibition of pollen tube growth occurred at ~1.5 nM LatB (Supplemental Fig. S5B). Together, these results suggest that the pollen germination and pollen tube growth of the *rmd-1* mutant are hypersensitive to LatB treatment.

Subsequently, we investigated the effect of LatB on actin filaments. The F-actin density and cables of both wild-type and *rmd-1* pollen tubes were decreased significantly compared with those of the control treatment with the application of 2 nM LatB (Fig. 5, F–H). However, *rmd-1* pollen tubes displayed more depolymerization of F-actin bundles compared with those of the wild type (Fig. 5, F and G). The wild-type pollen tube treated with LatB showed some random longitudinal actin bundles in the shank region, but no actin cables were observed in *rmd-1* pollen tubes treated with LatB, which is consistent with the statistical analysis of skewness (Fig. 5, F and H). These observations confirm that *rmd-1* pollen tubes are more sensitive to LatB treatment than wild-type pollen tubes, implying that RMD regulates pollen germination and pollen tube growth through stabilizing actin filaments.

RMD-Associated Actin Cables Modulate Pollen Tube Growth

To decipher how tip-localized RMD affects pollen tube growth and F-actin organization, we took advantage of tobacco pollen tubes because they are more robust and easily monitored for growth and cellular

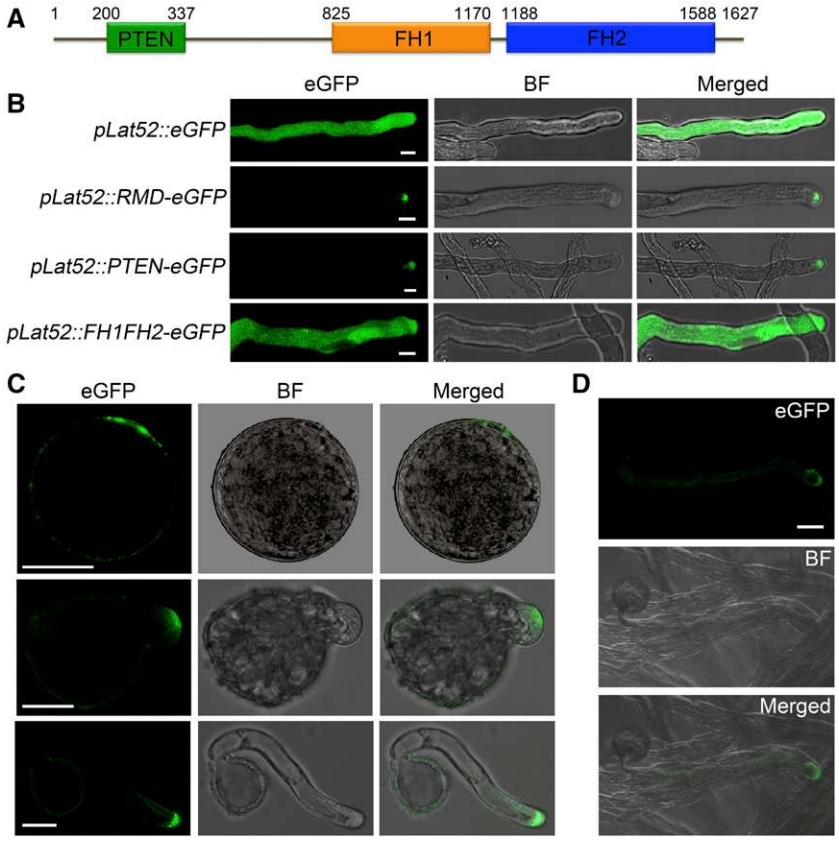

Figure 4. Subcellular localization of RMD in pollen tubes. A, Schematic representation of the predicted domain organization of RMD. Numbers indicate the amino acid positions of RMD. B, Representative confocal images of tobacco pollen tubes transiently expressing various versions of RMD fused with eGFP or single eGFP as a control driven by the pollen-specific *Lat52* promoter (*pLat52*). BF, Bright field. Bars = 10 μm. C and D, Localization of RMD in growing rice pollen tubes. Pollen grains from *rmd-1* plants expressing *RMD-eGFP* driven by the native *RMD* promoter (*proRMD::RMD-eGFP/rmd-1*) were germinated in vitro (C) and in vivo (D). Images show the RMD-eGFP signals in elongating pollen tubes in vitro (C) and tubes 10 min after pollination on the pistil in vivo (D). Bars = 20 μm.

structure in vitro. We coexpressed the F-actin marker Lifeact-mRFP with RMD-eGFP to visualize actin organization in growing pollen tubes, and all transgenes were expressed by the *Lat52* promoter. Transiently transformed pollen tubes showed that tip-localized RMD effectively drove the longitudinal actin cable in the shank region (Fig. 6A). Despite its tip localization, the expressed PTEN-like motif alone showed similar F-actin arrays to the expression of eGFP (control). However, the transiently expressed FH1FH2 domain of RMD resulted in a disordered F-actin organization and no obvious tip-accumulated GFP signal in the pollen tubes (Fig. 6A). These results suggest that both PTEN-mediated tip localization and FH1FH2-mediated actin binding of RMD are indispensable for the stability of the longitudinal actin cable in growing pollen tubes.

Furthermore, transient transformation assays showed that overexpression of full-length RMD could stimulate tobacco pollen tube growth (Fig. 6, A and B). However, overexpression of the PTEN-like motif or the FH1FH2 domain of RMD failed to enhance pollen tube length after 3 and 5 h of growth (Fig. 6, A and B). Notably, expression of the FH1FH2 domain of RMD significantly increased the pollen tube width in tobacco (Fig. 6, A and C), suggesting that the FH1FH2 domain of RMD without tip localization can cause defective polarized growth in pollen tubes. Consistently, overexpression of the FH1FH2 domains of *Saccharomyces cerevisiae* (yeast) and Arabidopsis formins caused defective polarity and growth arrest (Evangelista et al., 2002; Ye et al., 2009). Additionally, when pollen tubes were monitored individually during growth, the tubes with the transformed RMD-eGFP elongated at a higher rate (24.77 $\pm$ 3.83 nm s^{-1}; n = 16) compared with the control overexpressing only eGFP (20.15 $\pm$ 2.91 nm s^{-1}; n = 19; Fig. 6, D and E). These results demonstrate that tip-localized RMD plays a pivotal role in modulating pollen tube growth via modifying F-actin organization.

RMD Affects the Deposition of Pollen Tube Cell Wall Components

The observations that *rmd* mutants show shorter and wider pollen tubes rather than a cessation of growth imply that the cell expansion of *rmd* pollen tubes may be improperly guided. Pollen tube expansion depends on the deposition of newborn cell wall materials at the tip, and the deposited materials can be maintained by the polarized behaviors of F-actin (Rounds and Bezanilla, 2013; Rounds et al., 2014). To test whether the *rmd* pollen tube has a defective deposition of cell wall components, pectin labeling was performed with the carbohydrate antibody JIM5, which is used to indicate pectins with a low level of methylesterification (also called callose; Clausen et al., 2003). Immunofluorescence assays showed that the JIM5-labeled pectins were present along the shank of the tube and were excluded

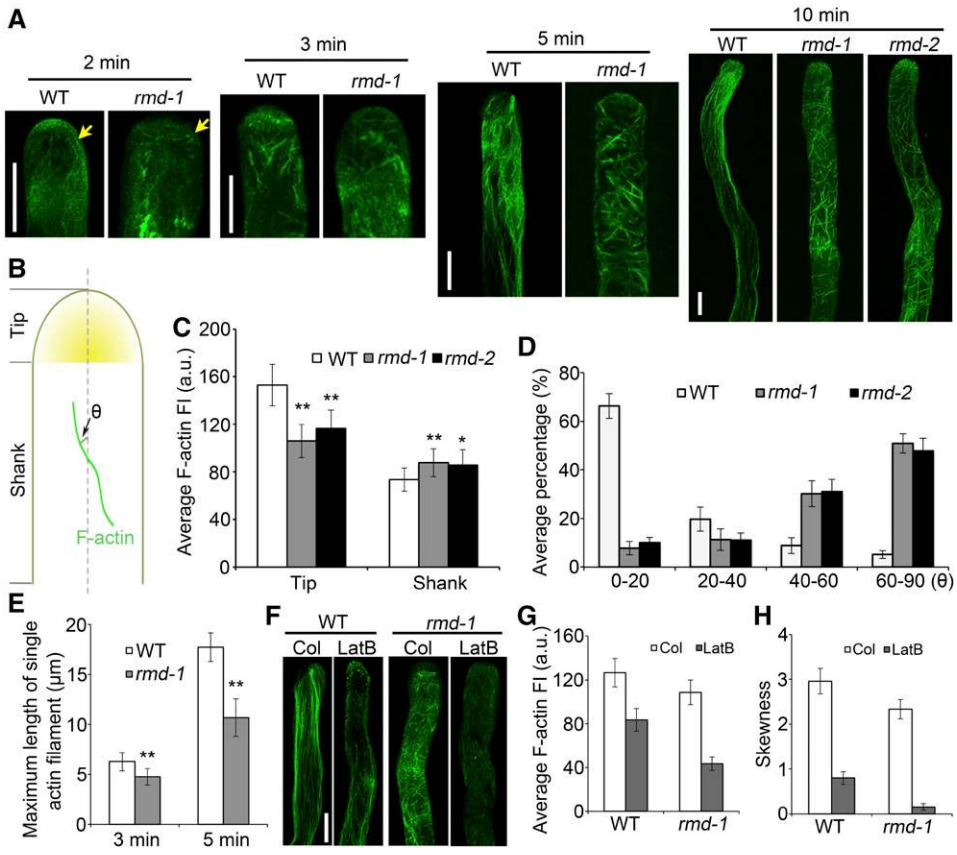

Figure 5. RMD determines the F-actin array orientation and distribution in rice pollen tubes. A, F-actin organization in growing pollen tubes. Wild-type (WT) and *rmd* pollen tubes were stained by Alexa Fluor 488-phalloidin 2, 3, 5, and 10 min after germination in vitro. Yellow arrows indicate the types of actin cables initiated in wild-type and *rmd-1* pollen tubes. Bars = 5 μm. B, Schematic diagram of actin filament arrays within the tip (apex and subapical zone) and shank region of pollen tubes. θ represents the net angle between the orientation of the F-actin array and the pollen tube growth axis. C, Average F-actin fluorescence intensity (FI) was measured at the tip and in the shank regions of wild-type ($n = 32$), *rmd-1* ($n = 36$), and *rmd-2* ($n = 31$) pollen tubes ($n > 30$ of each genotype). a.u., Arbitrary units. D, Average net angle distribution between actin cables and the pollen tube elongation axis. Actin cables visible in the shank of pollen tubes were selected, and the angles formed by each actin cable and the elongation axis were measured. More than 130 actin cables were analyzed for each genotype. Actin filaments of wild-type, *rmd-1*, and *rmd-2* pollen tubes were quantified 10 min after germination in vitro. E, The average maximum length of single tip-associated F-actin filaments was analyzed in wild-type and *rmd-1* pollen tubes. Pollen grains of the wild type and *rmd-1* mutants were germinated for 3 and 5 min in vitro, respectively. Approximately 100 actin filaments from 20 pollen tubes were monitored for each genotype. F, F-actin response to LatB in wild-type and *rmd-1* pollen tubes. Pollen grains were germinated under control (Col; DMSO) and 2 nM LatB conditions for 10 min. Bar = 5 μm. G, Average fluorescence intensity of F-actin in pollen tubes of the wild type ($n = 22$) and *rmd-1* ($n = 20$) in response to LatB as shown in F. H, F-actin bundling (skewness) analysis in pollen tubes of the wild type ($n = 22$) and *rmd-1* mutants ($n = 20$) in response to LatB as shown in F. All error bars represent SD of at least three experiments. Student's *t* test: *, $P < 0.05$ and **, $P < 0.01$.

from the apex of the wild-type pollen tube (Fig. 7, A and B; Supplemental Fig. S6A). However, JIM5-labeled signals were seen in both the shank and the apical regions of *rmd-1* and *rmd-2* pollen tubes (Fig. 7, A and B; Supplemental Fig. S6A), suggesting that the loss of function of *RMD* disrupts the distribution pattern of low-methylesterified pectins in growing pollen tube walls.

Additionally, another carbohydrate antibody, JIM7, was used to monitor the distribution of pectins with a high level of methylesterification (Clausen et al., 2003). In wild-type pollen tubes, the JIM7 antibody labeled a restricted section at the tip region (Fig. 7, C and D; Supplemental Fig. S6A). By contrast, in *rmd-1* and *rmd-2* pollen tubes, JIM7-labeled signals were observed among a more extensive region, including the apex and distal regions of the tube wall (Fig. 7, C and D; Supplemental Fig. S6A), suggesting that the *rmd* pollen tube has an altered deposition of pectin. Furthermore, Ruthenium Red, a specific dye for highly methylesterified pectins (Szumlanski and Nielsen, 2009), was introduced to analyze the cell wall components of the pollen tubes. In wild-type pollen tubes, Ruthenium Red bonded primarily with pectins at the

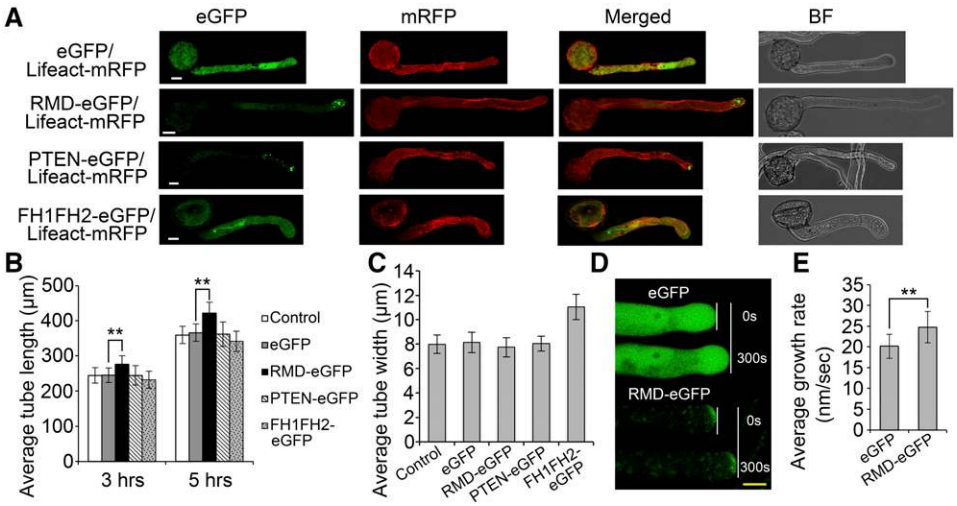

Figure 6. RMD-mediated F-actin organization regulates tobacco pollen tube growth. Data are from transiently transformed tobacco pollen tubes. All transgenes are expressed by the pollen-specific *Lat52* promoter. A, RMD-mediated F-actin organization contributes to tobacco pollen tube growth. Lifeact is an actin-binding protein to trace F-actin arrays (red signals). Images of pollen tubes were taken 3 h after germination. BF, Bright field. Bars = 10 μm. B, Growth response to RMD. Pollen tube length was measured 3 and 5 h as indicated after transformation with various versions of RMD fused with eGFP or single eGFP ($n > 40$ of each set). Control indicates wild-type tobacco pollen tubes. C, Statistics of pollen tube width as mentioned in B. Data were collected 3 h after transformation with various constructs in four independent experiments ($n > 40$ of each set). D, Contribution of RMD-eGFP and control (single eGFP) to pollen tube growth. White lines show the distance grown by the tubes in a comparable period (0–300 s). Yellow bar = 5 μm. E, Growth rate comparison. Growth rates were averaged from control (eGFP; $n = 16$) and RMD-eGFP ($n = 19$) tubes individually monitored for durations between 30 min and 1 h in three independent comparative experiments. All error bars represent SD of three biological repeats. Student's *t* test: **, $P < 0.01$.

tip of the pollen tube wall (Supplemental Fig. S6B), which is consistent with the immunolabeling assay using JIM7 antibody. By contrast, pollen tubes of *rmd* mutants and RNAi lines (*Ri-S*; Zhang et al., 2011) exhibited staining spots in the tip region as well as regions distal to the tip (Supplemental Fig. S6B). These results suggest that RMD is essential for the proper distribution of pectin with distinct properties in the pollen tube wall.

RMD Regulates the Efficiency of Cytoplasmic Streaming in Pollen Tubes

F-actin is believed to provide tracks for intracellular trafficking events, including cytoplasmic streaming, which also is defined as the coordinated flow of cytosol that carries small organelles and vesicles (Avisar et al., 2008; Ueda et al., 2010; Bloch et al., 2016). Therefore, the disorganization of actin filaments in *rmd* pollen tubes prompted us to speculate that RMD may affect cytoplasmic streaming. To test this, we observed that cytoplasmic streaming occurred in a reverse-fountain pattern in wild-type rice tubes (Supplemental Movie S1). Specifically, cytosolic organelles moved to the tip of the pollen tube by traveling along the cortex (red arrows) and then moved back in the reverse direction (green arrows) after reaching the tip (Fig. 8A). In contrast, the reverse-fountain pattern of cytoplasmic streaming was disrupted in *rmd-1* and *rmd-2* pollen tubes, and the movement of cytosolic organelles appeared random and irregular (Fig. 8B; Supplemental Movies S2 and S3). Cytosolic organelles moving in various directions were seen both in the shank and at the apex of *rmd-1* pollen tubes, and some cytosolic organelles showed oscillatory movement, suggesting the disordered pattern of cytoplasmic streaming in *rmd* pollen tubes.

Besides the analysis of cytoplasmic streaming, we observed the movement of cytosolic organelles to determine the speed of cytoplasmic streaming. Several independent pollen tubes were selected to determine the velocity of cytoplasmic streaming over a detectable distance (Fig. 8C; Supplemental Movies S1–S3). Statistical analysis showed that the velocity of cytoplasmic streaming was reduced significantly in *rmd-1* and *rmd-2* pollen tubes compared with that in the wild type (Fig. 8D; $n > 90$ organelles of each; $P < 0.01$). One intriguing phenotype was that some cytosolic organelles invaded at the extreme tip of *rmd* pollen tubes, leading to a loss of the clear zone normally found at the tip of wild-type tubes (Fig. 8E; Supplemental Fig. S7). Notably, the pattern and efficiency of cytoplasmic streaming in wild-type and *rmd-1* tubes were altered after treatment with LatB (Supplemental Movies S1, S2, S4, and S5), but the movement velocity of organelles in LatB-treated *rmd-1* pollen tubes seemed slower than that in the wild type (Supplemental Movies S4 and S5). Hence, we

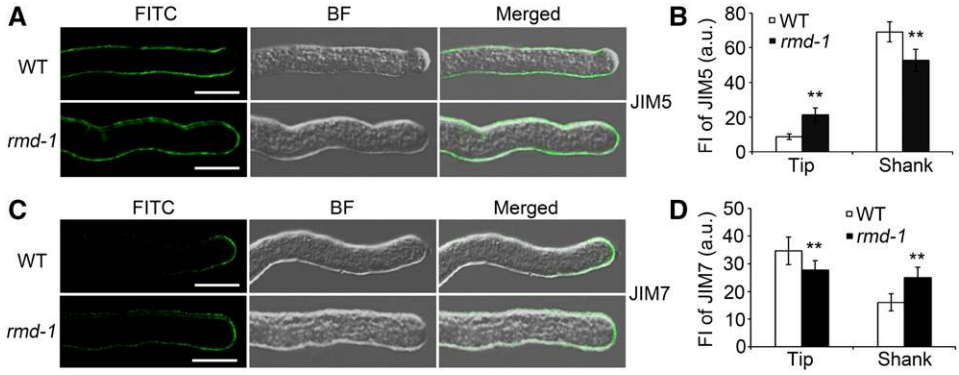

Figure 7. The *rmd-1* mutant has alterations in pollen tube cell wall composition. A, Wild-type (WT) and *rmd-1* pollen grains were germinated for 15 min, fixed, and labeled with the monoclonal antibody JIM5. Secondary antibodies were conjugated with FITC. BF, Bright field. Bars = 10 μm. B, Quantification analysis of JIM5 labeling in apical and shank zones of wild-type and *rmd-1* pollen tubes as mentioned in A ($n > 24$ of each genotype). a.u., Arbitrary units; FI, fluorescence intensity. C, Wild-type and *rmd-1* pollen grains were germinated for 15 min, fixed, and labeled with the monoclonal antibody JIM7. Secondary antibodies were conjugated with FITC. Bars = 10 μm. D, Quantification analysis of JIM7 labeling in apical and shank zones of wild-type and *rmd-1* pollen tubes as mentioned in C ($n > 20$ of each). All error bars represent SD of at least three independent experiments. Student's *t* test: **, $P < 0.01$.

concluded that RMD appears to play a key role in the positive regulation of cytoplasmic streaming efficiency and patterning during rice pollen tube growth.

DISCUSSION

In this study, we functionally characterized rice RMD, a type II formin, in regulating pollen tube growth. RMD modulates pollen germination and pollen tube elongation through the stabilization of actin filaments and the maintenance of these filaments as polarized arrays. Tip-localized RMD determines the distribution of methylesterified pectin along pollen tube cell walls and the pattern of cytoplasmic streaming in tubes (Fig. 9). Loss of function of *RMD* causes the disorganization of actin filaments in pollen grains and tubes, leading to abnormal pollen germination and retarded pollen tube growth. Thus, this study provides key molecular evidence demonstrating the function of a type II formin, RMD, in controlling tip growth by modifying actin organization in the model crop rice.

RMD Regulates Polarized Pollen Tube Growth

It is widely accepted that type I formins are essential for tip growth (Rounds and Bezanilla, 2013; van Gisbergen and Bezanilla, 2013). Overexpression of the actin-nucleating domain of the type I formin AtFH1 increases the number of actin cables in tobacco pollen tubes, exhibiting an initial growth rate increase followed by subsequent growth inhibition due to the accumulation of F-actin cables (Cheung and Wu, 2004). Arabidopsis FH3 and FH5 are critical for pollen tube growth via regulating F-actin nucleation (Ye et al., 2009; Cheung et al., 2010). In Arabidopsis root hairs, AtFH4 and AtFH8 regulate tip growth by modulating the accumulation of F-actin and actin-nucleating activity (Deeks et al., 2005; Yi et al., 2005). Lily LlFH1 regulates pollen tube growth and exocytic vesicles by modulating the formation of the actin fringe (Li et al., 2017). These observations suggest that type I formins affect tip growth through F-actin organization in plants. Additionally, Bni1p, a member of the formin family in yeast, exerts its effects on polarized morphogenesis and reorganization by regulating the actin cytoskeletal structure and activity (Evangelista et al., 1997, 2002). However, the role of type II formins in tip-growing cells remains unclear.

As a conserved type II formin member, RMD contains a PTEN-like motif at its N terminus, the poly-Pro-rich FH1 domain, and the FH2 domain as the characteristic features (Zhang et al., 2011). Here, we demonstrate the role of RMD in regulating pollen tube growth. First, RMD is abundantly expressed in pollen grains and pollen tubes (Fig. 3), which is consistent with the defects of the anther and pollen in *rmd* mutants. Subsequently, *rmd* mutants show delayed pollen germination and wider and shorter pollen tubes compared with the wild type. Additionally, overexpression of RMD significantly promotes tobacco pollen tube growth. These results demonstrate that RMD shares the conserved function of the type II formin family in pollen tube growth and polarity. Notably, RNAi of the type I formin NtFH5 in tobacco causes a severe phenotype showing drastically twisted and shortened pollen tubes compared with those of the *rmd* mutants (Cheung et al., 2010), suggesting the possible functional difference between type I and type II formins. Despite the decreased pollen activity in the *rmd* mutants, the mutant plants still manage to reproduce with a seed setting rate similar to that of the wild type, suggesting that *rmd* mutants may have normal female germ cells that do not have obvious abortion of pollination.

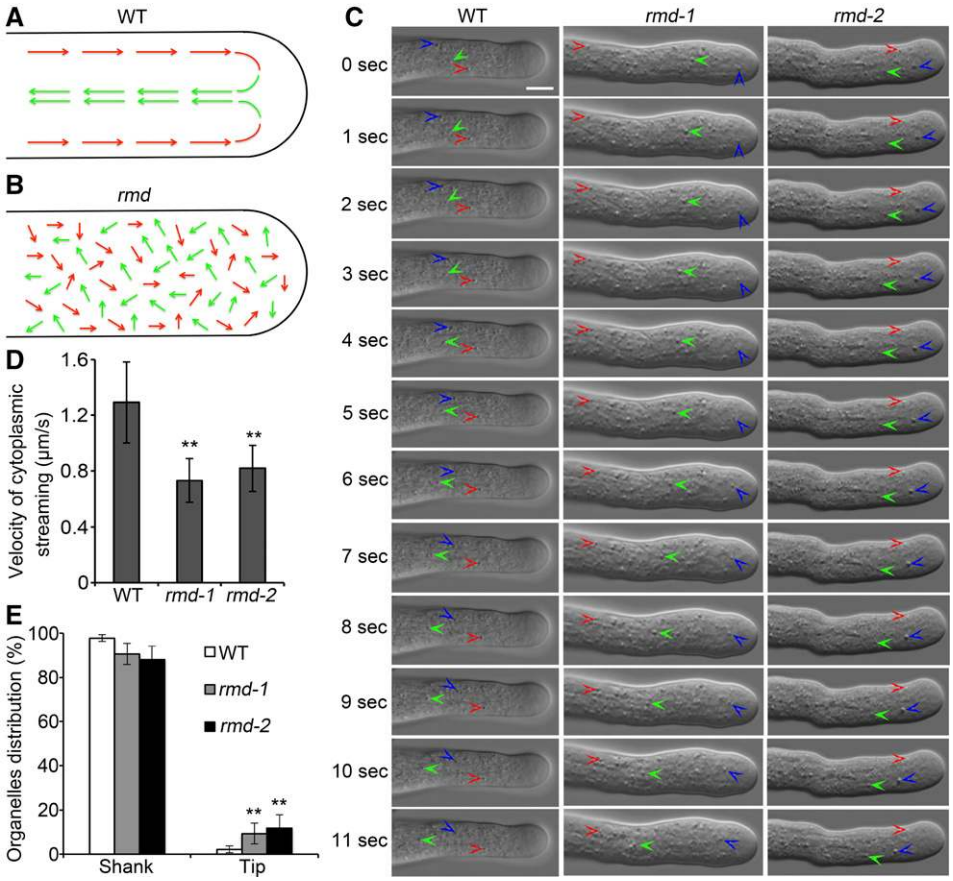

Figure 8. The pattern and velocity of cytoplasmic streaming are altered in *rmd* mutant pollen tubes. A and B, Schematic representations of cytoplasmic streaming patterns in wild-type (WT; A) and *rmd* (B) pollen tubes (Supplemental Movies S1–S3). Red and green arrows represent the directions of cytosolic organelles moving acropetally and basipetally, respectively. C, Single frames at 1-s intervals are shown (Supplemental Movies S1–S3). Three independent cytosolic organelles that showed continuous movement are labeled with three different colored arrowheads (red, green, and blue) in wild-type, *rmd-1*, and *rmd-2* pollen tubes. Bar = 5 μm. D, The velocity of cytoplasmic streaming was reduced significantly in *rmd-1* pollen tubes. Only the cytosolic organelles with continuous movement were selected for velocity analysis. More than 90 organelles from 15 pollen tubes of each genotype were measured. E, Distribution of organelles at the tip and in the shank of wild-type ($n = 26$), *rmd-1* ($n = 23$), and *rmd-2* ($n = 21$) pollen tubes. All visible organelles in whole tubes were counted. All error bars represent SD of at least three independent experiments. Student's *t* test: **, $P < 0.01$.

Tip Localization of RMD Is Essential for F-Actin Organization in Pollen Tubes

The F-actin network is thought to be intimately involved in the organization and function of the apical secretory machinery in promoting tip growth (Rounds and Bezanilla, 2013; Fu, 2015). In tip-growing cells, myosins drive the movement of Golgi-derived vesicles and other cell components along longitudinally oriented F-actin cables toward the growth region via cytoplasmic streaming (Hepler et al., 2001; Qu et al., 2017). Thus, one key role of F-actin in driving tip growth is to promote the long-distance movement of vesicles and organelles, transporting the raw materials for growth (plasma membrane and cell wall materials) toward the tip, which is required for the polarized growth and spatial patterning of tip-growing cells. Pollen tube growth is highly dependent upon the dynamic remodeling of the actin cytoskeleton (Gibbon et al., 1999; Hepler et al., 2001; Vidali et al., 2001; Rounds and Bezanilla, 2013; Fu, 2015).

Prompt and efficient disassociation of tip-nucleated actin filaments is critical for generating and maintaining the highly dynamic actin cytoskeleton in the pollen tube tip region (Cheung et al., 2010). In this work, we show that tip-localized RMD controls the actin network in pollen tube growth. *rmd* pollen grains have less obvious accumulation of F-actin during germination (Supplemental Fig. S4A). Clearly, *rmd* pollen tubes display the altered orientation of actin cables sharing the transverse F-actin organization in the shank region, and the dense actin structures also become disorganized both in the shank and at the apex of growing *rmd* pollen tubes (Fig. 5, A–D), resulting in a delay of pollen

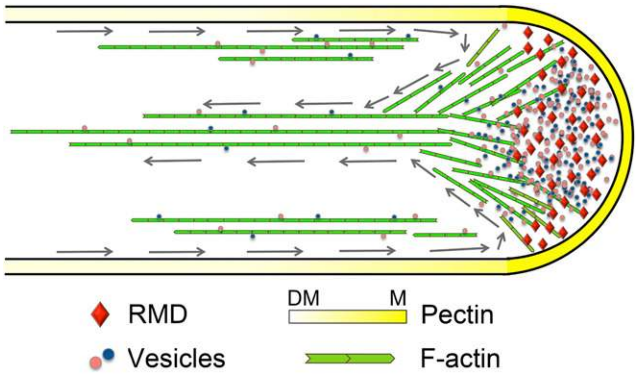

Figure 9. Model depicting the function of RMD in rice pollen tube growth. RMD, present at the tip of the pollen tube, functions as a key regulator that contributes to the F-actin-dependent maintenance of the spatial organization of cytoplasmic streaming, which is essential for pectin distribution to determine the tip growth of the rice pollen tube. Gray arrows trace the reverse-fountain cytoplasmic streaming pattern. DM, demethyl-esterified; M, methyl-esterified.

germination and the inhibition of pollen tube growth compared with that in the wild type. In addition, loss of function of *RMD* renders pollen tube growth, F-actin organization, and cytoplasmic streaming hypersensitive to the actin-depolymerizing drug LatB, further supporting the hypothesis that RMD is involved in pollen germination and tube growth via stabilizing actin filaments. Unlike RMD, AtFH5, a type I formin in Arabidopsis, stimulates actin assembly from the subapical membrane and stabilizes the subapical actin structure (Cheung et al., 2010), and Arabidopsis AtFH3 maintains the actin cables in the shank region. RNAi of *NtFH5* and *AtFH3* causes the abolished F-actin but no obvious change of F-actin direction in the shank region of pollen tubes (Ye et al., 2009; Cheung et al., 2010), suggesting that RMD may have distinct roles from those of type I formins in controlling F-actin polarity and distribution in pollen tubes.

Moreover, tip-localized RMD is guided by its PTEN-like domain. During pollen tube growth, the PTEN-like domain plays an important role in monitoring at the tip to maintain the organization and dynamics of actin. A study in the moss *P. patens* also demonstrated that the PTEN-like domain of the type II formin, For2A, targets to the apical region of growing cells (Vidali et al., 2009). Actin filament formation is initiated at the apical membrane of the tip region (Qu et al., 2017). Tip-localized RMD determines the direction of F-actin initiation from the PM (Fig. 5), which may further maintain the polarity of longitudinal F-actin cables in the shank region. We reasoned that RMD exerts its effects on F-actin cables through the initial direction of F-actin nucleation at the tip. In agreement with our previous data that the FH1FH2 domain of RMD has actin-nucleation activity and induces the bundling of actin filaments (Zhang et al., 2011), overexpression of RMD enhances the stability of longitudinal actin cables and the loss of function of *RMD* causes an altered density of actin structures and bundling polarity. However, without tip guiding directed by the RMD PTEN-like domain, overexpression of the FH1FH2 domain results in a depolarized growth of tobacco pollen tubes (Fig. 6, A–C). Together, RMD localizes at the tip and binds the elongating actin filaments from the membrane to control the polarized nucleation direction of F-actin. Elongated F-actin is guided to the cytoplasm of the shank region and maintains polarized cables as the originating orientation. Therefore, RMD positively contributes to the establishment and polarity of the F-actin network during rice pollen tube growth.

Notably, both type I and type II formins have been demonstrated to accelerate actin elongation in the presence of plant profilins (Zhang et al., 2016b; Li et al., 2017). In Arabidopsis, profilins act as important players in regulating polarized pollen tube growth by modulating actin polymerization at the apical membrane (Liu et al., 2015). Our previous studies also demonstrated that RMD FH1FH2 could effectively nucleate actin polymerization from the actin/profilin complex (Zhang et al., 2011), but the mechanism of RMD/profiling-coordinated F-actin activity in rice pollen tube growth remains to be further elucidated. Besides binding to actin filaments, our previous study showed that RMD also is a microtubule-stabilizing protein (Zhang et al., 2011). Several previous investigations showed that treatment with the microtubule-depolymerizing chemical oryzalin causes no obvious effect on pollen tube growth (Bou Daher and Geitmann, 2011; Zhou et al., 2015), suggesting a minimal function of microtubules on pollen tube growth (Cai et al., 1997). In addition, unlike the role of formins in nucleating the unbranched actin filaments, the actin-related protein2/3 (ARP2/3) complex is known to form a branched actin network (Cheung and Wu, 2004). During Arabidopsis leaf trichome morphogenesis, the ARP2/3-generated actin meshwork and a microtubule-depletion zone are required for cell wall assembly to maintain the length of the elongating trichome branch (Yanagisawa et al., 2015), indicating the cooperation of the apical actin meshwork and the microtubule cytoskeleton in the establishment of cell wall pattern and shape. The differentiated function in tip growth regulation between the ARP2/3 complex and formins is likely to result from the different manners of actin nucleation.

RMD Controls Cytoplasmic Streaming and Cell Wall Components during Pollen Tube Growth

It is accepted that the actomyosin system can power vesicle trafficking and cytoplasmic streaming (Avisar et al., 2008; Cai et al., 2015; Fu, 2015; Qu et al., 2017). In this context, the organization of vesicle trafficking and cytoplasmic streaming mirrors the arrangement of F-actin (Chen et al., 2007; Cheung et al., 2010). The observation of *rmd* pollen tubes showing an altered efficiency of cytoplasmic streaming is thought to be due to

the disorganized and depolarized F-actin arrays and cables at the tip and in the shank, respectively.

In *rmd* pollen tubes, one of the most significant phenotypes is the absence of the reverse-fountain cytoplasmic streaming pattern, which is seen in the wild type. Supportively, longitudinal actin cables, which provide the stability and polarity of molecular tracks for cytoplasmic streaming, are altered in the shank region of *rmd* pollen tubes. Besides the changes of cytoplasmic streaming, the velocity of the movement of organelles is decreased significantly in *rmd-1* pollen tubes, which is associated with the altered distribution of organelles (Fig. 8, D and E), implying that defects of F-actin arrangement and dynamics impair myosin-based particle movement. This is consistent with the phenotype of RNAi of type I formin *AtFH3* pollen tubes in Arabidopsis (Ye et al., 2009).

Massive secretion during cell wall formation at the pollen tube tip is critical for the incorporation of materials into the apical plasma membrane, which are subsequently retrieved by endocytic membrane recycling and cytoplasmic streaming movement (Rojas et al., 2011; Chebli et al., 2012; Grebnev et al., 2017). The pollen tube wall has a unique organization, with the growing tip consisting mainly of pectin and the flanks containing a callose layer (Bosch and Hepler, 2005). We observed that, in *rmd* pollen tubes, the distribution of pectin is no longer present exclusively in the growing tip. We also show that callose is not only present along the flanks of *rmd* pollen tubes, as it is in the wild type, but also protrudes into the tip. This suggests that loss of function of *RMD* may affect the trafficking of pectin and callose. Pectin distribution is required for the formation of pollen tubes with a normal appearance, and the disruption of a single pectin methylesterase frequently causes severe pollen tube defects (Tian et al., 2006; Rounds and Bezanilla, 2013), suggesting that the altered deposition of pectin in the pollen tube wall of *rmd* mutants also causes abnormal pollen tube growth.

In short, this study shows that RMD, a type II formin, is required for pollen tube growth by regulating the organization and array polarity of apical and shank F-actin in rice (Fig. 9). RMD localizes at the internal tip of pollen tubes and determines the F-actin density at the apex and the array orientation and polarity of longitudinal actin cables in the shank. RMD-associated F-actin characteristics are critical for maintaining the proper pattern of cytoplasmic streaming, which determines the pollen tube tip-distributed pectin, directing the polar growth of pollen tubes.

MATERIALS AND METHODS

Plant Material and Growth Conditions

The *rmd-1* and *rmd-2* mutants, the *RMD* RNAi line *Ri-S*, and the *proRMD*::*GUS* transgenic rice (*Oryza sativa*) lines have been described previously (Zhang et al., 2011; Li et al., 2014). The complementary line was created by expressing *RMD-eGFP* driven by its own promoter in the *rmd-1* background. To generate the *proRMD*::*RMD-GFP* construct, the 3,000-bp promoter and cDNA fragment of *RMD* was cloned into the *pCAMBIA3301* vector using an infusion kit (primers proR-F, 5′-GCAGGCATGCAAGCTTACGGGATAGTACGATGGTGGG-3′; proR-R, 5′-CTCACCATTACCATGGCCTTCCCCTCCTCCTCCTCC-3′; cR-F, 5′-GCTGTACAAGAGATCTATGGCGCTCTTCCGCAAATTCTTC-3′; and cR-R, 5′-TGCTCACCATACTAGTACCTACATCTTTTCCTCGTCTGC-3′). The construct was introduced into the *rmd-1* mutant by *Agrobacterium tumefaciens*-mediated transformation as described previously (Li et al., 2006). At least 15 independent positive lines were analyzed for pollen tubes. The background of all rice plants used in this study is the *japonica* type cv 9522 (Zhang et al., 2011). Mature rice plants were grown in the paddy field, as described previously (Zhang et al., 2011; Li et al., 2014), as well as in the greenhouse of Waite Campus (University of Adelaide). Tobacco (*Nicotiana tabacum*) plants were grown in growth chambers at 25°C under natural light with daylight extension to 16 h.

In Vitro Pollen Germination and Pollen Tube Growth

Rice pollen grains from at least 10 plants were collected by gently shaking panicles in the paddy field or greenhouse during anthesis. These fresh pollen grains were transferred into a liquid germination medium [20% (w/v) Suc, 10% (v/v) polyethylene glycol 4000, 3 mM $Ca(NO_3)_2 \cdot 4H_2O$, 40 mg L^{-1} H_3BO_3, and 3 mg L^{-1} vitamin B1] and cultured for about 1 to 10 min at room temperature (30°C) under moist conditions to generate synchronously germinated rice pollen grains. To investigate the effect of the actin-depolymerizing chemical LatB on pollen tube growth, various concentrations of LatB were added to the germination medium. The amount of germinated rice pollen grains and the morphological characteristics of pollen tubes were examined using a Nikon E600 microscope and a Nikon DXM1200 digital camera. The localization of RMD in rice pollen tubes was observed using a Leica TCS SP5 confocal laser scanning microscope equipped with a ×63, 1.46 numerical aperture (NA) HC PLAN objective lens. To calculate the germination percentage, a minimum of 200 pollen grains was counted in each experiment. To calculate average pollen tube length and width, at least 150 pollen tubes were measured using ImageJ (http://rsbweb.nih.gov/ij/; version 1.38) in each experiment. At least three experiments were conducted. The observations of reproductive organs and the activity of pollen grains were performed as described by Li et al. (2006), and the lengths of the anther and pistil were measured using the ImageJ tool.

Aniline Blue Staining of Pollen Tubes in Vivo

Aniline Blue staining of pollen tubes in pistils was performed as described previously with slight modifications (Ishiguro et al., 2001). Briefly, decolorized Aniline Blue solution was prepared by making a 0.1% (w/v) solution of Aniline Blue (Acros Organics), adding 1 M NaOH drop-wise, and incubating the solution overnight at 48°C until it became a transparent yellow color. Following in vivo pollination, preemasculated mature wild-type flowers were pollinated with wild-type, *rmd-1*, or *rmd-2* pollen. After 10, 20, and 30 min, the pollinated pistils were removed from the plants and incubated in fixing solution containing ethanol:acetic acid (3:1) for 2 h at room temperature. The fixed pistils were then washed with distilled water three times for 5 min each followed by incubation in 1 M NaOH softening solution overnight. Pistils were placed into decolorized Aniline Blue solution and allowed to stain for 12 to 24 h before being mounted on slides and observed using a Leica SP5 microscope with a ×10 objective and 405-nm laser line excitation. Emission spectra were collected from 440 to 612 nm. Z stacks were taken through specimens.

RMD Expression Analysis

To evaluate the expression of *RMD* in reproductive organs, lemmas, paleas, lodicules, pistils, anthers, and whole flowers of wild-type rice were collected separately and frozen in liquid nitrogen. About 20 mg of pollen was harvested and frozen in liquid nitrogen. Total RNA was extracted from each sample using Trizol reagent (Invitrogen). cDNA was synthesized from each RNA sample using a reverse transcription kit (Fermentas) according to the instructions. *UBIQUITIN* was used to equalize the amounts of cDNA from the different sources. The SYBR Green qRT-PCR Mix (Bio-Rad) was used for RT-qPCR on a CFX96 (Bio-Rad) machine. The primers, reaction conditions, and programs for RT-qPCR and semiquantitative RT-PCR were described previously (Li et al., 2014).

The pistils, anthers, pollen grains, and pollen tubes of wild-type plants stably transformed with the *pCAMBIA-proRMD*::*GUS* fusion construct were stained for GUS activity as described previously (Zhang et al., 2011; Li et al., 2014). The images were taken using a Leica light microscope (DFC402C) with a camera.

DNA Manipulation and Plasmid Construction

All plasmids used for transient expression in tobacco (*Nicotiana tabacum*) pollen were constructed in the *pLat52* vector (kindly provided by Zhenbiao Yang) as described previously (Fu et al., 2001). cDNA of *RMD* was amplified by PCR with gene-specific primers (5′-TACCATGGAGTCTAGAATGGCGCT-CTTCCGCAAATTCTTC-3′ and 5′-ATATCTCCTTGGATCCAACCTACAT-CTTTTCCTCGTCTGC-3′) and cloned into a *pLat52*::*eGFP* vector using an infusion kit. Subsequently, the fragments of the PTEN-like domain (primers 5′-TACCATGGAGTCTAGAATGAGCCGACCCCTCATCTTGG-3′ and 5′-ATA-TCTCCTTGGATCCAAGGGTCTGAAAAGACTACCTC-3′) and the FH1FH2 domain (primers 5′-TACCATGGAGTCTAGAATGCCTCCACCTCCACCTCCAC-3′ and 5′-ATATCTCCTTGGATCCACTTTTCTGCTTCTGCCTCTT-3′) were amplified by PCR from *RMD* cDNA and cloned into the *pLat52*::*eGFP* vector. For particle bombardment, all plasmids were amplified in *Escherichia coli* strain Top10 and purified using plasmid Midi kits according to the manufacturer's instructions (Qiagen).

Particle Bombardment-Mediated Transient Expression in Tobacco Pollen

Mature tobacco pollen grains were used for transient expression with a particle bombardment procedure as described previously (Fu et al., 2001; Wang and Jiang, 2011). Briefly, tobacco pollen grains were collected immediately before each experiment and suspended in a pollen germination medium containing 0.01% (w/v) boric acid, 1 mM $CaCl_2$, 1 mM $Ca(NO_3)_2 \cdot 4H_2O$, 1 mM $MgSO_4 \cdot 7H_2O$, and 10% (w/v) Suc (pH 6.5). A drop of 80 to 100 μL of medium containing pollen grains from several flowers was applied to a piece of nylon membrane (Micron Separations) placed on top of a piece of 90-mm filter paper (Whatman) in a 100- × 15-mm petri dish. Once the liquid was drained from the membrane, an additional 1.5 mL of pollen germination medium was added to the filter paper. Pollen grains were then immediately bombarded with DNA-coated gold particles using a PDS-1000/He particle-delivery system (Bio-Rad). The settings of the PDS-1000/He particle-delivery system were as follows: 1,100 p.s.i., 29 mm Hg vacuum, 1-cm gap distance between the rupture disk and the macrocarrier, and 6-cm particle flight distance between the macrocarrier and pollen grain samples.

Gold particles (1 μm diameter) were coated with plasmid DNA according to the manufacturer's procedures (Bio-Rad) immediately before bombardment. For investigating the colocalization of RMD with F-actin, 0.5 μg of *pLat52*::*eGFP* (control), *pLat52*::*RMD-eGFP*, *pLat52*::*PTEN-eGFP*, or *pLat52*::*FH1FH2-eGFP* plasmid DNA was used with 1 μg of *pLat52*::*Lifeact-mRFP* (kindly provided by Haiyun Ren) plasmid DNA each. Bombarded pollen grains were incubated in pollen germination medium at room temperature for 4 h before observation using a Leica TCS SP5 confocal laser scanning microscope equipped with a ×63, 1.46 NA HC PLAN objective. Fluorescence signals were visualized with 488-nm laser excitation and emission at 500 to 570 nm for GFP and with 543-nm laser excitation and emission at 580 to 630 nm for RFP.

F-Actin Staining and Quantification

The actin cytoskeleton was visualized according to previously described methods with slight modifications (Zhang et al., 2011; Li et al., 2014). Briefly, pollen grains and pollen tubes were spread on the surface of pollen germination medium and fixed for 1 h in 300 μM 3-maleimidobenzoic acid *N*-hydroxysuccinimide ester in liquid pollen germination medium. The pollen grains were extracted subsequently with 0.05% Nonidet P-40 in liquid germination medium for 10 min. Fixed pollen grains and pollen tubes were incubated in PEM buffer (100 mM PIPES, 10 mM EGTA, 5 mM MgSO4, and 0.3 M mannitol, pH 6.9) that contained 2% (w/v) glycerol (Sigma-Aldrich) and 6.6 μM Alexa Fluor 488-phalloidin staining (Invitrogen). Images were collected with a Leica TCS SP5 confocal laser scanning microscope equipped with a ×63, 1.46 NA HC PLAN objective. The fluorescent phalloidin was excited using the 488-nm line of an argon laser, and optical sections were scanned and captured.

The angles formed between each actin cable and the growth axes of individual pollen tubes were analyzed using ImageJ. Curled pollen tubes were excluded from this analysis because their growth axes were difficult to define. As actin cables were nearly parallel to the growth axis in the shanks of wild-type pollen tubes, only this region was used for quantification. For each pollen tube, three to four optical sections were excluded between sections used for analysis to ensure that each actin cable was analyzed only once. For wave-like actin cables that formed more than one angle with the growth axis, only the largest angle was used for quantification. The average fluorescence intensity and actin bundles (skewness) were performed as described previously (Zhang et al., 2011; Li et al., 2014).

Immunolabeling of Pollen Tubes

The fluorescence labeling method was modified from a previously described protocol using Arabidopsis (*Arabidopsis thaliana*) plants (Szumlanski and Nielsen, 2009). Rice pollen tubes were filtered and subsequently fixed by the addition of 5% (v/v) paraformaldehyde in liquid germination medium for 30 min. The fixation was quenched for 15 min by the addition of 50 mM ammonium chloride in germination medium. The pollen was washed three times with pollen germination medium and blocked for 1 h in 3% (w/v) milk in germination medium. The carbohydrate antibody JIM5 or JIM7 (CarboSource) was diluted 1:200 in germination medium containing 3% (w/v) milk. The pollen was incubated for 1 h in the primary antibody, washed three times with 3% (w/v) milk in germination medium, and incubated for 1 h in 1:200 anti-rat IgG conjugated to FITC (Sigma-Aldrich) diluted in 3% (w/v) milk in germination medium. The pollen was washed three times with germination medium and viewed using a Leica TCS SP5 confocal laser scanning microscope equipped with a ×63, 1.46 NA HC PLAN objective, a 491-nm excitation laser, and a 535-nm emission filter. Z stacks (2 mm thickness) were taken through each specimen.

ImageJ software was used for fluorescence quantification of the labeled cell wall components (pectin and callose). Pixel intensity was measured along the periphery of each pollen tube, beginning from the pole. Values for fluorescence intensity were normalized to the highest fluorescence value for individual tubes before averaging ($n > 20$ for each sample).

Ruthenium Red Staining of Pollen Tubes

The germinated pollen was stained by Ruthenium Red (Sigma-Aldrich), which was dissolved in rice pollen germination medium at a final concentration of 0.01% (w/v; Szumlanski and Nielsen, 2009). After staining for 10 to 15 min, images were collected using a Nikon E600 microscope and a Nikon DXM1200 digital camera.

Analysis of Cytoplasmic Streaming

Wild-type and mutant pollen grains were germinated for 3 to 10 min as described above. Time-lapse images of cytoplasmic streaming were collected at 1-s intervals using a Leica TCS SP5 microscope with differential interference contrast optics equipped with a ×63, 1.46 NA HC PLAN objective. A minimum of 40 cytosolic organelles from at least 10 pollen tubes were selected randomly for the determination of cytoplasmic streaming velocity in each replicate, and at least three replicates were conducted. Only cytosolic organelles undergoing continuous movements were selected for velocity analysis. The distance traveled by a selected cytosolic organelle during a given time was determined with ImageJ.

Accession Number

The accession number for *RMD* (*OsFH5*) is Os07g0596300.

Supplemental Data

The following supplemental materials are available.

Supplemental Figure S1. RMD is essential for anther and pistil development and pollen activity in rice.

Supplemental Figure S2. Loss of function of *RMD* causes the repressed elongation of pollen tubes.

Supplemental Figure S3. Defective pollen tube growth in *rmd-2* mutant.

Supplemental Figure S4. RMD is required for F-actin organization in rice pollen grains and pollen tubes.

Supplemental Figure S5. Loss of function of *RMD* increases the sensitivity to LatB in pollen germination and pollen tube growth.

Supplemental Figure S6. Loss of function of *RMD* leads to abnormal pectin distribution in pollen tube cell wall.

Supplemental Figure S7. Organelles shown at the tip of *rmd* pollen tubes.

Supplemental Movie S1. Cytoplasmic streaming in the wild-type pollen tube.

Supplemental Movie S2. Cytoplasmic streaming in the *rmd-1* pollen tube.

Supplemental Movie S3. Cytoplasmic streaming in the *rmd-2* pollen tube.

Supplemental Movie S4. Cytoplasmic streaming in the wild-type pollen tube treatment with LatB.

Supplemental Movie S5. Cytoplasmic streaming in the *rmd-1* pollen tube treatment with LatB.

ACKNOWLEDGMENTS

We thank Zhenbiao Yang (University of California, Riverside) for providing the *pLat52*::*eGFP* vector and Haiyun Ren (Beijing Normal University) for providing the *pLat52*::*Lifeact-mRFP* F-actin marker. We thank Deborah Devis (University of Adelaide) for revision and comments on the article.

Received January 9, 2018; accepted March 19, 2018; published March 26, 2018.

LITERATURE CITED

Avisar D, Prokhnevsky AI, Makarova KS, Koonin EV, Dolja VV (2008) Myosin XI-K is required for rapid trafficking of Golgi stacks, peroxisomes, and mitochondria in leaf cells of *Nicotiana benthamiana*. Plant Physiol **146:** 1098–1108

Berepiki A, Lichius A, Read ND (2011) Actin organization and dynamics in filamentous fungi. Nat Rev Microbiol **9:** 876–887

Bloch D, Pleskot R, Pejchar P, Potocký M, Trpkošová P, Cwiklik L, Vukašinović N, Sternberg H, Yalovsky S, Žárský V (2016) Exocyst SEC3 and phosphoinositides define sites of exocytosis in pollen tube initiation and growth. Plant Physiol **172:** 980–1002

Bosch M, Hepler PK (2005) Pectin methylesterases and pectin dynamics in pollen tubes. Plant Cell **17:** 3219–3226

Bou Daher F, Geitmann A (2011) Actin is involved in pollen tube tropism through redefining the spatial targeting of secretory vesicles. Traffic **12:** 1537–1551

Cai G, Cresti M (2009) Organelle motility in the pollen tube: a tale of 20 years. J Exp Bot **60:** 495–508

Cai G, Moscatelli A, Cresti M (1997) Cytoskeletal organization and pollen tube growth. Trends Plant Sci **2:** 86–91

Cai G, Parrotta L, Cresti M (2015) Organelle trafficking, the cytoskeleton, and pollen tube growth. J Integr Plant Biol **57:** 63–78

Chebli Y, Kaneda M, Zerzour R, Geitmann A (2012) The cell wall of the Arabidopsis pollen tube: spatial distribution, recycling, and network formation of polysaccharides. Plant Physiol **160:** 1940–1955

Chen CY, Wong EI, Vidali L, Estavillo A, Hepler PK, Wu HM, Cheung AY (2002) The regulation of actin organization by actin-depolymerizing factor in elongating pollen tubes. Plant Cell **14:** 2175–2190

Chen T, Teng N, Wu X, Wang Y, Tang W, Šamaj J, Baluška F, Lin J (2007) Disruption of actin filaments by latrunculin B affects cell wall construction in *Picea meyeri* pollen tube by disturbing vesicle trafficking. Plant Cell Physiol **48:** 19–30

Cheung AY, Niroomand S, Zou Y, Wu HM (2010) A transmembrane formin nucleates subapical actin assembly and controls tip-focused growth in pollen tubes. Proc Natl Acad Sci USA **107:** 16390–16395

Cheung AY, Wu HM (2004) Overexpression of an *Arabidopsis* formin stimulates supernumerary actin cable formation from pollen tube cell membrane. Plant Cell **16:** 257–269

Cheung AY, Wu HM (2008) Structural and signaling networks for the polar cell growth machinery in pollen tubes. Annu Rev Plant Biol **59:** 547–572

Clausen MH, Willats WGT, Knox JP (2003) Synthetic methyl hexagalacturonate hapten inhibitors of anti-homogalacturonan monoclonal antibodies LM7, JIM5 and JIM7. Carbohydr Res **338:** 1797–1800

Deeks MJ, Cvrcková F, Machesky LM, Mikitová V, Ketelaar T, Zársky V, Davies B, Hussey PJ (2005) *Arabidopsis* group Ie formins localize to specific cell membrane domains, interact with actin-binding proteins and cause defects in cell expansion upon aberrant expression. New Phytol **168:** 529–540

Duckney P, Deeks MJ, Dixon MR, Kroon J, Hawkins TJ, Hussey PJ (2017) Actin-membrane interactions mediated by NETWORKED2 in Arabidopsis pollen tubes through associations with Pollen Receptor-Like Kinase 4 and 5. New Phytol **216:** 1170–1180

Evangelista M, Blundell K, Longtine MS, Chow CJ, Adames N, Pringle JR, Peter M, Boone C (1997) Bni1p, a yeast formin linking cdc42p and the actin cytoskeleton during polarized morphogenesis. Science **276:** 118–122

Evangelista M, Pruyne D, Amberg DC, Boone C, Bretscher A (2002) Formins direct Arp2/3-independent actin filament assembly to polarize cell growth in yeast. Nat Cell Biol **4:** 32–41

Fu Y (2015) The cytoskeleton in the pollen tube. Curr Opin Plant Biol **28:** 111–119

Fu Y, Wu G, Yang Z (2001) Rop GTPase-dependent dynamics of tip-localized F-actin controls tip growth in pollen tubes. J Cell Biol **152:** 1019–1032

Geitmann A, Emons AMC (2000) The cytoskeleton in plant and fungal cell tip growth. J Microsc **198:** 218–245

Geitmann A, Steer M (2006) The architecture and properties of the pollen tube cell wall. *In* R Malhó, ed, The Pollen Tube: A Cellular and Molecular Retrospective. Plant Cell Monographs, **Vol 3**. Springer-Verlag, Berlin, pp 177–200

Gibbon BC, Kovar DR, Staiger CJ (1999) Latrunculin B has different effects on pollen germination and tube growth. Plant Cell **11:** 2349–2363

Grebnev G, Ntefidou M, Kost B (2017) Secretion and endocytosis in pollen tubes: models of tip growth in the spot light. Front Plant Sci **8:** 154

Hepler PK, Vidali L, Cheung AY (2001) Polarized cell growth in higher plants. Annu Rev Cell Dev Biol **17:** 159–187

Hepler PK, Winship LJ (2015) The pollen tube clear zone: clues to the mechanism of polarized growth. J Integr Plant Biol **57:** 79–92

Ishiguro S, Kawai-Oda A, Ueda J, Nishida I, Okada K (2001) The *DEFECTIVE IN ANTHER DEHISCIENCE* gene encodes a novel phospholipase A1 catalyzing the initial step of jasmonic acid biosynthesis, which synchronizes pollen maturation, anther dehiscence, and flower opening in *Arabidopsis*. Plant Cell **13:** 2191–2209

Lee YJ, Yang Z (2008) Tip growth: signaling in the apical dome. Curr Opin Plant Biol **11:** 662–671

Li G, Liang W, Zhang X, Ren H, Hu J, Bennett MJ, Zhang D (2014) Rice actin-binding protein RMD is a key link in the auxin-actin regulatory loop that controls cell growth. Proc Natl Acad Sci USA **111:** 10377–10382

Li N, Zhang DS, Liu HS, Yin CS, Li XX, Liang WQ, Yuan Z, Xu B, Chu HW, Wang J, et al (2006) The rice *tapetum degeneration retardation* gene is required for tapetum degradation and anther development. Plant Cell **18:** 2999–3014

Li S, Dong H, Pei W, Liu C, Zhang S, Sun T, Xue X, Ren H (2017) LlFH1-mediated interaction between actin fringe and exocytic vesicles is involved in pollen tube tip growth. New Phytol **214:** 745–761

Liu X, Qu X, Jiang Y, Chang M, Zhang R, Wu Y, Fu Y, Huang S (2015) Profilin regulates apical actin polymerization to control polarized pollen tube growth. Mol Plant **8:** 1694–1709

Lovy-Wheeler A, Wilsen KL, Baskin TI, Hepler PK (2005) Enhanced fixation reveals the apical cortical fringe of actin filaments as a consistent feature of the pollen tube. Planta **221:** 95–104

Lowery LA, Van Vactor D (2009) The trip of the tip: understanding the growth cone machinery. Nat Rev Mol Cell Biol **10:** 332–343

McKenna ST, Kunkel JG, Bosch M, Rounds CM, Vidali L, Winship LJ, Hepler PK (2009) Exocytosis precedes and predicts the increase in growth in oscillating pollen tubes. Plant Cell **21:** 3026–3040

Qu X, Jiang Y, Chang M, Liu X, Zhang R, Huang S (2015) Organization and regulation of the actin cytoskeleton in the pollen tube. Front Plant Sci **5:** 786

Qu X, Zhang H, Xie Y, Wang J, Chen N, Huang S (2013) *Arabidopsis* villins promote actin turnover at pollen tube tips and facilitate the construction of actin collars. Plant Cell **25:** 1803–1817

Qu X, Zhang R, Zhang M, Diao M, Xue Y, Huang S (2017) Organizational innovation of apical actin filaments drives rapid pollen tube growth and turning. Mol Plant **10:** 930–947

Ren H, Xiang Y (2007) The function of actin-binding proteins in pollen tube growth. Protoplasma **230:** 171–182

Rojas ER, Hotton S, Dumais J (2011) Chemically mediated mechanical expansion of the pollen tube cell wall. Biophys J **101:** 1844–1853

Rounds CM, Bezanilla M (2013) Growth mechanisms in tip-growing plant cells. Annu Rev Plant Biol **64:** 243–265

Rounds CM, Hepler PK, Winship LJ (2014) The apical actin fringe contributes to localized cell wall deposition and polarized growth in the lily pollen tube. Plant Physiol **166:** 139–151

Staiger CJ, Poulter NS, Henty JL, Franklin-Tong VE, Blanchoin L (2010) Regulation of actin dynamics by actin-binding proteins in pollen. J Exp Bot **61:** 1969–1986

Su H, Zhu J, Cai C, Pei W, Wang J, Dong H, Ren H (2012) FIMBRIN1 is involved in lily pollen tube growth by stabilizing the actin fringe. Plant Cell **24:** 4539–4554

Szumlanski AL, Nielsen E (2009) The Rab GTPase RabA4d regulates pollen tube tip growth in *Arabidopsis thaliana*. Plant Cell **21:** 526–544

Tian GW, Chen MH, Zaltsman A, Citovsky V (2006) Pollen-specific pectin methylesterase involved in pollen tube growth. Dev Biol **294:** 83–91

Twell D, Klein TM, Fromm ME, McCormick S (1989) Transient expression of chimeric genes delivered into pollen by microprojectile bombardment. Plant Physiol **91:** 1270–1274

Ueda H, Yokota E, Kutsuna N, Shimada T, Tamura K, Shimmen T, Hasezawa S, Dolja VV, Hara-Nishimura I (2010) Myosin-dependent endoplasmic reticulum motility and F-actin organization in plant cells. Proc Natl Acad Sci USA **107:** 6894–6899

van Gisbergen PA, Bezanilla M (2013) Plant formins: membrane anchors for actin polymerization. Trends Cell Biol **23:** 227–233

van Gisbergen PA, Li M, Wu SZ, Bezanilla M (2012) Class II formin targeting to the cell cortex by binding PI(3,5)P(2) is essential for polarized growth. J Cell Biol **198:** 235–250

Vidali L, McKenna ST, Hepler PK (2001) Actin polymerization is essential for pollen tube growth. Mol Biol Cell **12:** 2534–2545

Vidali L, van Gisbergen PA, Guérin C, Franco P, Li M, Burkart GM, Augustine RC, Blanchoin L, Bezanilla M (2009) Rapid formin-mediated actin-filament elongation is essential for polarized plant cell growth. Proc Natl Acad Sci USA **106:** 13341–13346

Wang H, Jiang L (2011) Transient expression and analysis of fluorescent reporter proteins in plant pollen tubes. Nat Protoc **6:** 419–426

Wang J, Xue X, Ren H (2012) New insights into the role of plant formins: regulating the organization of the actin and microtubule cytoskeleton. Protoplasma **249:** S101–S107

Winship LJ, Obermeyer G, Geitmann A, Hepler PK (2010) Under pressure, cell walls set the pace. Trends Plant Sci **15:** 363–369

Wu Y, Yan J, Zhang R, Qu X, Ren S, Chen N, Huang S (2010) *Arabidopsis* FIMBRIN5, an actin bundling factor, is required for pollen germination and pollen tube growth. Plant Cell **22:** 3745–3763

Yanagisawa M, Desyatova AS, Belteton SA, Mallery EL, Turner JA, Szymanski DB (2015) Patterning mechanisms of cytoskeletal and cell wall systems during leaf trichome morphogenesis. Nat Plants **1:** 15014

Yang W, Ren S, Zhang X, Gao M, Ye S, Qi Y, Zheng Y, Wang J, Zeng L, Li Q, et al (2011) *BENT UPPERMOST INTERNODE1* encodes the class II formin FH5 crucial for actin organization and rice development. Plant Cell **23:** 661–680

Ye J, Zheng Y, Yan A, Chen N, Wang Z, Huang S, Yang Z (2009) *Arabidopsis* formin3 directs the formation of actin cables and polarized growth in pollen tubes. Plant Cell **21:** 3868–3884

Yi K, Guo C, Chen D, Zhao B, Yang B, Ren H (2005) Cloning and functional characterization of a formin-like protein (AtFH8) from Arabidopsis. Plant Physiol **138:** 1071–1082

Zerzour R, Kroeger J, Geitmann A (2009) Polar growth in pollen tubes is associated with spatially confined dynamic changes in cell mechanical properties. Dev Biol **334:** 437–446

Zhang M, Zhang R, Qu X, Huang S (2016a) *Arabidopsis* FIM5 decorates apical actin filaments and regulates their organization in the pollen tube. J Exp Bot **67:** 3407–3417

Zhang S, Liu C, Wang J, Ren Z, Staiger CJ, Ren H (2016b) A processive *Arabidopsis* formin modulates actin-filament dynamics in association with profilin. Mol Plant **9:** 900–910

Zhang Z, Zhang Y, Tan H, Wang Y, Li G, Liang W, Yuan Z, Hu J, Ren H, Zhang D (2011) *RICE MORPHOLOGY DETERMINANT* encodes the type II formin FH5 and regulates rice morphogenesis. Plant Cell **23:** 681–700

Zheng Y, Xie Y, Jiang Y, Qu X, Huang S (2013) *Arabidopsis* actin-depolymerizing factor7 severs actin filaments and regulates actin cable turnover to promote normal pollen tube growth. Plant Cell **25:** 3405–3423

Zhou Z, Shi H, Chen B, Zhang R, Huang S, Fu Y (2015) *Arabidopsis* RIC1 severs actin filaments at the apex to regulate pollen tube growth. Plant Cell **27:** 1140–1161